Formation of an Organized Monolayer by Solution Adsorption of Octadecyltrichlorosilane on Gold: Electrochemical Properties and Structural Characterization

H. O. Finklea,* L. R. Robinson, A. Blackburn, and B. Richter

Department of Chemistry, Virginia Polytechnic Institute and State University, Blackburg, Virginia 24061

D. Allara* and T. Bright

Bell Communications Research, Murray Hill, New Jersey 07974

Received September 26, 1985. In Final Form: December 12, 1985

An organized hydrophobic monolayer is formed on smooth zero-valent gold by adsorption of octadecyltrichlorosilane (OTS) from a hexadecane solution. Wetting properties, infrared (IR) spectra, and ellipsometry measurements are consistent with the silyl moiety adjacent to the metal surface and with an all-trans conformation hydrocarbon chain extended vertically from the surface with a small average tilt. The silyl head groups appear to be incorporated into a two-dimensional cross-linked network of Si–O–Si bonds within the monolayer. However, polymerization is not complete as suggested by IR and Auger spectra which indicate the presence of SiOH groups and residual Cl, respectively. Electrochemical measurements indicate the monolayer-covered gold surface behaves as a blocked electrode containing pinhole defects. Conditions for film formation on Pt were also investigated for comparison.

Introduction

Organized monolayers on surfaces are an elegant approach to designing molecular structures with known spacings and orientation.[1,2] An organized monolayer is constructed by using a bifunctional molecule, usually a small head group with an affinity for the substrate combined with a long hydrocarbon tail. Typical examples include fatty acids and alcohols deposited on glass and metal substrates. Two method of deposition are (1) the classic Langmuir–Blodgett method,[3,4] in which the molecules are spread on an air–water interface, compressed, and transferred to the solid substrate, and (2) the adsorption method,[5] in which the molecules spontaneously assemble on the surface from solution.

There is clearly a need to explore fundamental aspects of organized monolayers on surfaces because of important technological and fundamental applications. Of particular interest to us is the potential ability to precisely control electrochemical processes by the control of monolayer structure on the electrode surface. For example, electron-transfer rates are expected to be strong functions of monolayer thickness, packing density, and molecular orientation. The search for such important structure–property correlations have been the impetus for a number of previous studies of monolayer-coated electrodes. The majority of these studies concern molecules adsorbed on mercury[6–16] or platinum[17–23] in the presence of free solute molecules. Less common are reports of oriented monolayers deposited prior to the electrochemistry,[24–27] especially on solid metal electrodes.[28,29] Predeposited monolayers provide the advantages of being characterizable ex situ and offer wide ranges of preparative procedures.

Octadecyltrichlorosilane (OTS) forms monolayers on oxidized aluminum, oxidized silicon, and glass substrates.[30–36] Adsorption of OTS from a nonpolar liquid[30–32]

(1) Mobius, D. *Ber. Bunsenges. Phys. Chem.* **1978**, *82*, 848–858.
(2) Whitten, D. G.; Eaker, D. W.; Horsey, B. E.; Schmehl, R. H.; Worsham, P. R. *Ber. Bunsenges. Phys. Chem.* **1978**, *82*, 858–867.
(3) Blodgett, K. B. *J. Am. Chem. Soc.* **1935**, *57*, 1007–1022.
(4) Blodgett, K. B.; Langmuir, I. *Phys. Rev.* **1937**, *51*, 964–982.
(5) Bigelow, W. C.; Pickett, D. L.; Zisman, W. A. *J. Colloid Sci.* **1946**, *1*, 513.
(6) Lipkowski, J.; Kosinska, E.; Goledzinowski, M.; Nieniewska, J., Galus, Z. *J. Electroanal. Chem.* **1975**, *59*, 344–349.
(7) Goledzinowski, M.; Kisova, L.; Lipkowski, J.; Galus, Z. *J. Electroanal. Chem.* **1979**, *95*, 43–57.
(8) Lipkowski, J.; Galus, Z. *J. Electroanal. Chem.* **1979**, *98*, 91–104.
(9) Pyzik, G.; Lipkowski, J. *J. Electroanal. Chem.* **1981**, *123*, 351–364.
(10) Muller, E.; Emons, H.; Dorfler, H.-D.; Lipkowski, J. *J. Electroanal. Chem.* **1982**, *142*, 39–55.
(11) Buess-Herman, Cl.; Quarin, G.; Gierst, L.; Lipkowski, J. *J. Electroanal. Chem.* **1983**, *148*, 79–95.
(12) Blank, M.; Miller, I. R. *J. Colloid Interface Sci.* **1968**, *26*, 26–33.
(13) Miller, I. R.; Blank, M. *J. Colloid Interface Sci.* **1968**, *26*, 34–40.
(14) Pezzatini, G.; Foresti, M. L.; Guidelli, R. *J. Electroanal. Chem.* **1982**, *138*, 139–153.
(15) Pezzatini, G.; Mariani, P.; Guidelli, R. *J. Electroanal. Chem.* **1985**, *185*, 315–329.
(16) Jehring, H.; Retter, U.; Horn, E. *J. Electroanal. Chem.* **1983**, *149*, 153–166.
(17) Lane, R. F.; Hubbard, A. T. *J. Phys. Chem.* **1973**, *77*, 1401–1410.
(18) Lane, R. F.; Hubbard, A. T. *J. Phys. Chem.* **1973**, *77*, 1411–1421.
(19) Soriaga, M.; Hubbard, A. T. *J. Am. Chem. Soc.* **1982**, *104*, 3937–3945.
(20) Soriaga, M.; Wilson, P. H.; Hubbard A. T., Benton, C. S. *J. Electroanal. Chem.* **1982**, *142*, 317–336.
(21) Soriaga, M.; Stickney, J. L.; Hubbard, A. T. *J. Electroanal. Chem.* **1983**, *144*, 207–215.
(22) Soriaga, M.; Hubbard, A. T. *J. Electroanal. Chem.* **1983**, *159*, 101–116.
(23) White, J. H.; Soriaga, M.; Hubbard, A. T. *J. Electroanal. Chem.* **1985**, *185*, 331–338.
(24) Memming, R. *Discuss. Faraday Soc.* **1974**, *58*, 262–271.
(25) Arden, W.; Fromherz, P. *Ber. Bunsenges. Phys. Chem.* **1978**, *82*, 868–874.
(26) Fromherz, P.; Arden, W. *J. Am. Chem. Soc.* **1980**, *102*, 6211–6218.
(27) Daifuku, H.; Aoki, K.; Tokuda, K.; Matsuda, H. *J. Electroanal. Chem.* **1982**, *140*, 179–185.
(28) Laitinen, H. A.; Chao, M. S. *Anal. Chem.* **1961**, *33*, 1836–1838.
(29) Li, T. T.-T.; Liu, H. Y.; Weaver, M. J. *J. Am. Chem. Soc.* **1984**, *106*, 1233–1239.
(30) Polymeropoulos, E. E.; Sagiv, J. *J. Chem. Phys.* **1978**, *69*, 1836–1847.
(31) Sagiv, J. *Isr. J. Chem.* **1979**, *78*, 339–345, 346–353.
(32) Sagiv, J. *J. Am. Chem. Soc.* **1980**, *102*, 92–98.
(33) Netzer, L.; Iscovici, R.; Sagiv, J. *Thin Solid Films* **1983**, *99*, 235–241.

0743-7463/86/2402-0239$01.50/0

is a more successful approach for monolayer synthesis than the Langmuir–Blodgett method.[35] Its success appears to arise in part from the ability of the trichlorosilyl head group to react with substrate surface hydroxyls to form siloxy bonds. The latter chemistry has been used to bond many different silanes to metal and nonmetal electrodes.[37] Strong bonding of the head group to the substrate is normally anticipated to be essential to stable monolayers during electrochemistry.

However, the functionalization of a nonreactive electrode such as gold presents some problems in terms of finding film attachment processes. For example, palmitic acid monolayers readily wash off gold electrodes.[28] Because of the reactivity of gold oxide, covalent bonding of adsorbate to any oxide which one can electrochemically form would probably possess an inherent instability of the interface. As an alternative approach, one might conceive of two-dimensional polymeric networks which would form strong attachments because of the well-known entropically based stability of polymer monolayers to dissolution. The OTS molecule appears to be an appropriate candidate for forming such a layer because of the presence of three potential cross-link sites in each head group.

The focus of this paper is to report the interesting observation that OTS, in fact, can be deposited in monolayer quantities on a zero-valent gold electrode by an ex-situ solution deposition technique. The application of electrochemical, ellipsometric, contact angle, and infrared spectroscopic measurements demonstrates that a stable, oriented, cross-linked, monolayer forms which although densely packed is not completely defect-free.

Experimental Section

Gold- and platinum-coated glass slides (1 × 3 cm) (Evaporated Metal Films, Inc.) were composed of 1000 Å of the respective metal evaporated on top of 50 Å of a TiO_2 binding layer. Most experiments were performed on gold electrodes. Oxide-stripping experiments were also performed on gold flag electrodes. Four pretreatments were used to clean and prepare the electrode surface for monolayer deposition: (A) dipping the electrode in hot H_2O_2/H_2SO_4 (1:10) for 10 s, (B) immersing the electrode in 0.5 M H_2SO_4 and cycling its potential between −0.25 and +1.40 V vs. SCE, (C) immersing the electrode in 0.1 M NaOH and cycling its potential between −1.00 and +.70 V vs. SCE, and (D) dipping the electrode briefly in 0.1 M NaOH. All pretreatments were followed by copious rinsing with deionized water and drying with an air stream. For pretreatments B and C, potential cycling was continued until a steady-state voltammogram characteristic of the clean metal was obtained. The cleaning scans ended with the metal in the reduced state. Oxide layers were obtained by anodizing the electrode near the oxygen evolution potential for 1–5 min. Anodized electrodes were hydrophilic, while consistent hydrophilicity was observed only for oxide-free electrodes cycled in base. Since truly clean gold and platinum are hydrophilic,[38] pretreatment C was judged to be the most suitable before monolayer deposition.

Rinse and electrolyte water were obtained from a Barnstead Nanopure Deionizer. OTS (Petrarch Systems, Inc.) was vacuum-distilled and stored in a drybox. Hexadecane was passed through a column of activated alumina until it did not spread on a water–air interface.[5] Deposition solutions (ca. 0.1 M) were prepared by mixing 0.40 mL of OTS with 10.0 mL of hexadecane inside the drybox and then bringing the solutions out to the bench top. Following electrochemical cleaning, rinsing, and drying at room temperature, electrodes were dipped into the stirred solution for 5 min and carefully removed. Some electrodes were immediately dipped in chloroform, with no visible difference in the results. The usable lifetime of the solutions was approximately 1 h, at which point a faint film of siloxane polymer was visible on the surface.

Electrochemistry was performed in a conventional three-electrode cell by using argon sparging. Film thicknesses were determined by using two different Rudolph 423 null ellipsometers. Further details of the apparatus and calculation details are given elsewhere.[39] Infrared spectra were obtained by a single reflection at a glancing angle (~4° off glancing) on a modified Digilab 15B Fourier transform spectrometer. Experimental details can be found in an earlier report.[40] The sample was mounted in a nitrogen-purged box isolated from the rest of the spectrometer system by KBr windows. Determination of the optical constants of pure, liquid-phase OTS were made by using internal reflection measurements on a thick film (≳several μm) formed on a ZnSe prism. The calculations were made using standard parallel layer theory.[40]

Results

Formation of the Monolayer. Successful deposition only occurs when the gold surface is immersed in an OTS solution immediately after it has been water-rinsed and dried. If the sample is transported to a drybox for the deposition process no well-formed monolayer results. Both anodized and oxide-free metal surfaces exhibit this property. We hypothesize that the OTS molecules are assembling on a thin film of water (several monolayers, perhaps) covering the substrate rather than on the substrate itself. The surface oxide appears to be unnecessary for OTS monolayer formation on Pt and Au and, in the case of Au, actually detrimental to the coverage and stability of the monolayer.

In the case of an OTS monolayer formed on an oxidized-gold surface, evidence below suggests that the deposition processes removes the oxide to leave a gold–monolayer interface. The amount of reducible oxide formed on a gold surface is measured in an oxide-stripping voltammogram, as shown in Figure 1 for gold and platinum. The freshly anodized gold shows a double peak assignable to surface oxide (+.81 V) and bulk oxide reduction (+.77 V).[41] The gold oxide layer is relatively reactive; immersion of a freshly anodized electrode in pure hexadecane (a "blank" reaction) results in a 50% loss of strippable oxide (Q = 5.2 mC/cm^2 for the freshly anodized electrode and 2.7 mC/cm^2 for the "blank" reaction). However, a gold electrode that has been coated with an OTS monolayer exhibits no visible oxide strippping peak (Q < 0.2 mC/cm^2). A similar result is obtained if the oxide stripping is performed in acetonitrile (Figure 1B). Trichloromethylsilane likewise removes any trace of strippable oxide. The latter result suggests that $SiCl_3$ moieties initially reduce the gold oxide. Electrochemical oxidation of chloromethylsilanes is known.[42] XPS spectra before and after silanization support the loss of the gold oxide.[43] Hence the final OTS monolayer is formed on an oxide-free gold surface.

In contrast, a strippable oxide is retained on platinum following OTS deposition (Figure 1C). The relevant quantities of strippable oxide are 1.6 mC/cm^2 for a freshly anodized electrode, 0.67 mC/cm^2 for an electrode that has also been immersed in hexadecane, and 0.41 mC/cm^2 for

(34) Netzer, L.; Iscovici, R.; Sagiv, J. *Thin Solid Films* **1983**, *100*, 67–76.
(35) Maoz, R.; Sagiv, J. *J. Colloid Interface Sci.* **1984**, *100*, 465–496.
(36) Gun, J.; Iscovici, R.; Sagiv, J. *J. Colloid Interface Sci* **1984**, *101*, 201–213.
(37) Murray, R. W. *Acc. Chem. Res.* **1980**, *13*, 135.
(38) Smith, T. *J. Colloid Interface Sci.* **1980**, *75*, 51.
(39) Allara, D. L.; Nuzzo, R. G. *Langmuir* **1985**, *1*, 45–52.
(40) Allara, D. L.; Nuzzo, R. G. *Langmuir* **1985**, *1*, 52–66.
(41) Rand, D. A. J.; Woods, R. *J. Electroanal. Chem.* **1971**, *31*, 29–38.
(42) Allred, A. L.; Bradley, C.; Newman, T. H. *J. Am. Chem. Soc.* **1978**, *100*, 5081–5084.
(43) Fischer, A. B.; Wrighton, M. S.; Umana, M., Murray, R. W. *J. Am. Chem. Soc.* **1979**, *101*, 3442–3446.

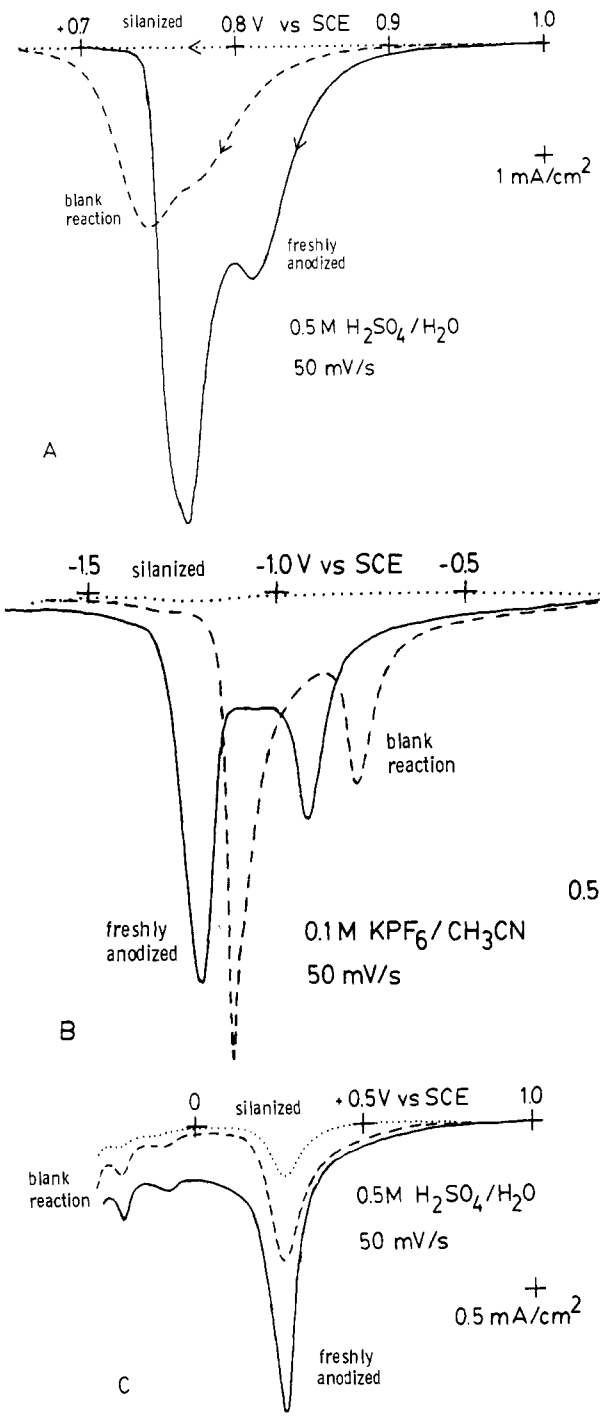

Figure 1. Electrochemical stripping of (A) gold oxide in 0.5 M H_2SO_4, (B) gold oxide in 0.1 M KPF_6/CH_3CN, and (C) platinum oxide in 0.5 M H_2SO_4. All electrodes were anodized in 0.5 M H_2SO_4 for 300 s at +1.80 V vs. SCE (gold) or +1.60 V vs. SCE (platinum). See text for details.

the OTS-coated Pt electrode. Facci and Murray[44] also reported retention of a fraction of strippable oxide following the reaction of anodized Pt electrodes with chlorosilanes. They concluded that bonding of silanes to the surface oxide layer passivates it toward reduction. This contradicts the Pt(4f) XPS spectra, which show no measureable "PtO" phase after silanization.[43,44]

For both gold and platinum electrodes, there is no direct evidence of bonding between the OTS monolayer and the surface metal oxide. Since OTS monolayers assemble on

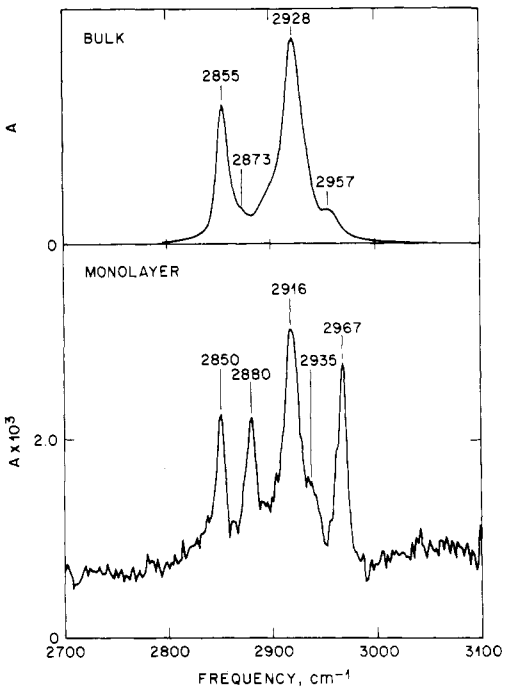

Figure 2. Infrared transmission and reflection spectra of bulk liquid OTS and a monolayer on gold, respectively, for the CH stretching region. Spectral intensity units are absorbance defined for the reflection spectrum as -log R/R_0 where R = sample reflectivity and R_0 = reflectivity of a clean gold reference.

oxide-free surfaces, most of the following results are obtained with nonanodized electrodes.

Characterization of the Monolayer. The wetting properties of the coated electrodes are consistent with a close-packed monolayer with the terminal methyl groups exposed.[28,32] Hexadecane, chloroform, acetonitrile, methanol, and water do not wet the surface of the electrode, while hexane does. Contact angles (static) are 111.3 ± 2.3° and 37.8 ± 0.9° for water and hexadecane, respectively.

Two independent sets of measurements with different ellipsometers yield the same thickness for OTS monolayers: 30 ± 3 Å, assuming an index of refraction of approximately 1.45 for the monolayer. Justification of the assumed index of refraction is based on the comparable densities and indices of refraction for OTS (d = 0.95 g/cm³; n_D = 1.45) and alkylsiloxane polymer (d = 0.90–0.96 g/cm³; n_D = 1.41–1.43). The thickness is appropriate for a single layer with a fully extended hydrocarbon chain oriented vertically to the surface.[30] Multilayers or three-dimensional polymer networks are ruled out.

Detailed evidence for the above structure is provided by grazing angle infrared spectroscopy (Figure 2 and 3). In Figure 2 the C–H stretching region of the monolayer spectrum shows four easily discernable peaks: 2850, 2880, 2916, and 2967 cm⁻¹. These are assigned respectively to the following stretching modes: CH_2 symmetric ($d^+(\pi)$), CH_3 symmetric (r^+), CH_2 asymmetric ($d^-(\pi)$), and CH_3 asymmetric (in plane of CCC backbone, r_a^-). The mode symbols are given in parentheses.[45] Also barely discernable is a shoulder at ~2935 cm⁻¹ which is assigned to a Fermi resonance mode of the CH_3 group in analogy with previous assignments of long-chain n-alkanoic acid monolayers.[40] For comparison, a spectrum of bulk OTS is shown also in Figure 2. Mode assignments[40] for discernable peaks in this spectrum are the following: $d^+(\pi)$, 2855 cm⁻¹; r^+, 2873 cm⁻¹; $d^-(\pi)$, 2928 cm⁻¹; r_0^- (CH_3 asymmetric stretch

(44) Facci, J. S.; Murray, R. W. *J. Electroanal. Chem.* **1980**, *112*, 221.

(45) Snyder, R. G.; Hsu, S. L.; Krimm, S. *Spectrochim. Acta, Part A* **1978**, *34A*, 395–406.

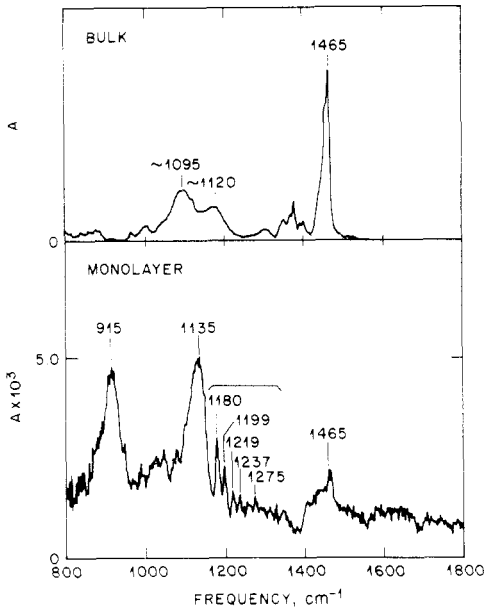

Figure 3. Same as in Figure 2 but for the mid-IR region 800–1800 cm^{-1}.

out of plane to CCC backbone), 2957 cm^{-1}. Important differences between the monolayer and bulk spectra in the C–H stretch region exist. First, the relative intensities are widely different. The monolayer spectrum is similar to that of a chemisorbed monolayer of *n*-hexadecanoic acid on oxidized aluminum.[40] The structure of the latter has been interpreted[40] in terms of an assembly of alkyl chains extending away from the surface with an average tilt of about 12° and a twist of about 45° for an all trans zigzag extended chain. Since the all-trans extended conformation is valid (see evidence below) for the OTS monolayer, an average tilted structure, similar to the *n*-hexadecanoic acid on oxidized aluminum, can be assigned. Detailed calculations, using optical constant data for pure OTS, in fact show an average chain tilt of 15–20° with an approximate 45° twist to the chain. The latter twist can be interpreted in terms of unaligned domains of tipped chains.

The second important difference between the bulk and monolayer is the relative positions of the C–H stretch modes. In particular, the $d^+(\pi)$ CH_2 modes are shifted 5 and 12 cm^{-1} to lower frequencies, respectively, in the monolayer relative to the bulk. Differences of this magnitude and direction are expected between conformationally ordered (crystalline) and disordered (liquid) phases.[46] Since the bulk OTS sample is liquid it seems appropriate to conclude that the monolayer is extensively ordered conformationally.

The lower frequency spectra are shown in Figure 3. Assignments for the monolayer spectrum area are 915 cm^{-1}, Si–OH stretch (or SiO–H bend), 1135 cm^{-1}, Si–O–Si stretch, 1180, 1199, 1219, 1237, and 1275 cm^{-1}, wag–twist progression; and 1465 cm^{-1}, CH_2 scissors bending. For comparison, a transmission spectrum of a bulk liquid is shown in Figure 3. The CH_2 bending mode appears at 1465 cm^{-1}. There are a number of small peaks which have not been assigned. However, two features should be noted. First, there is no evidence for the wag–twist progression seen in the monolayer. This is not surpprising since the sample is in the liquid state. Second, the two large broad bands at ~1095 and ~1120 cm^{-1} are probably due to Si–O stretching modes caused by limited hydrolysis since no

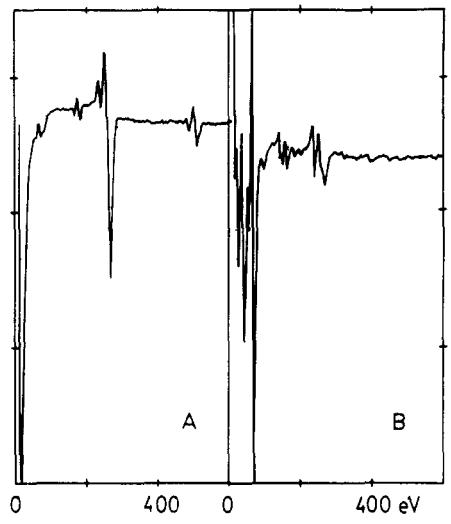

Figure 4. Auger spectroscopy of a coated electrode before (A) and after (B) argon ion sputtering. The vertical scaling is different for the two spectra. The sputtering beam (4 kV, 0.2 μA) was rastered over a 4 × 4 mm area for 5 min.

particular precautions were taken to prepare and handle the sample in a dry environment. In general, the Si–O stretching modes in a variety of silicon compounds[47] occur over nearly a 200-cm^{-1} region with most values centered in the range 1000–1100 cm^{-1}. However, the monolayer spectrum does not appear similar to the partially hydrolyzed bulk sample (air exposed) but rather very similar to that reported[48] for medium alkyl chain length oligomeric alkylhydroxysiloxanes, formed by extensive hydrolysis of the corresponding alkyltrichlorosilanes. For example,[48] $[C_8H_{17}SiO(OH)]_6$ exhibits a moderately strong band at 900 cm^{-1} and an intense broad band at 1130 cm^{-1}. The similar C_7 oligimer shows corresponding absorptions at 980 and ~1140–1185 cm^{-1}, while the similar C_6 oligmer shows absorptions at 890 and 1075–1100 cm^{-1}. In this series the 890–980-cm^{-1} bands were shown to associated with the Si–OH groups[48] whereas the ~1100-cm^{-1} region bands were present whether Si–OH was present or not. Thus it seems clear in the case of the monolayer that extensively polymerized networks of Si–O–Si bonds are formed with some proportion of Si–OH groups. The weak intensity CH_2 bending mode peak at 1465 cm^{-1} is consistent with a vertically oriented chain. This conclusion follows from the IR surface selection rule[40] since the transition moment for this mode is in the CH_2 plane which should be close to parallel to the gold surface. The wag–twist progression with ~18-cm^{-1} intervals is direct evidence for fully extended alkyl chains with all-trans conformations. The observed splitting pattern is quite consistent with previous reports of these modes in medium-chain alkyl groups.[49-52]

Auger spectroscopy of an OTS-coated electrode (Figure 4A) shows the presence of gold (72 eV), chlorine (182 eV), carbon (272 eV), and oxygen (512 eV). Silicon is not visible even at high resolution. Chlorine suggests the presence of unreacted Si–Cl groups or perhaps adsorbed HCl, the byproduct of Si–Cl hydrolysis. A rastering argon ion

(46) Snyder, R. G.; Strauss, H. L.; Elliger, C. A. *J. Phys. Chem.* **1982**, *86*, 5145–5150.

(47) For example, see: Bellamy, L. J. "The Infrared Spectra of Complex Molecules"; Wiley: New York, 1975; and references cited therein.

(48) Andrianov, K. A.; Izmaylov, B. A. *J. Organomet. Chem.* **1967**, *8*, 435–441.

(49) Holland, R. F.; Nielsen, J. L. *J. Mol. Spectrosc.* **1926**, *8*, 383–405.

(50) Jones, R. N.; McKay, A. F.; Sinclair, R. G. *J. Am. Chem. Soc.* **1952**, *74*, 2575–2578.

(51) Meiklejohn, R. A.; Meyer, R. J.; Avonovic, S. M.; Scheutte, H. A.; Maloc, V. W. *Anal. Chem.* **1957**, *29*, 329–334.

(52) Synder, R. G.; Schactschneider, J. H. *Spectrochim. Acta* **1963**, *19*, 85–116.

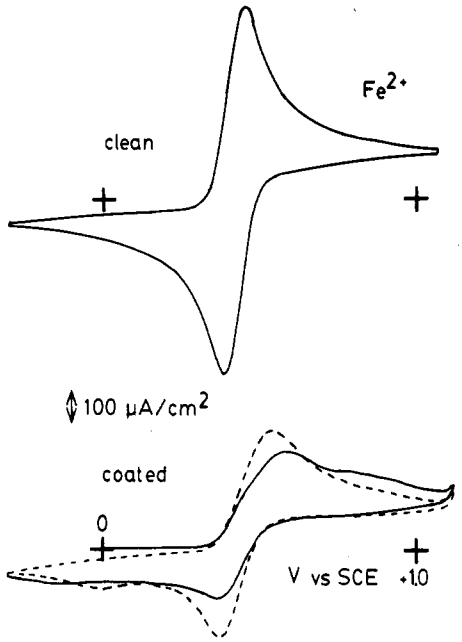

Figure 5. Cyclic voltammetry of a clean and a coated electrode. 2.0 mM Fe^{2+} in 0.5 M H_2SO_4; sweep rate 50 mV/s. Solid line, first scan; dashed line, second scan.

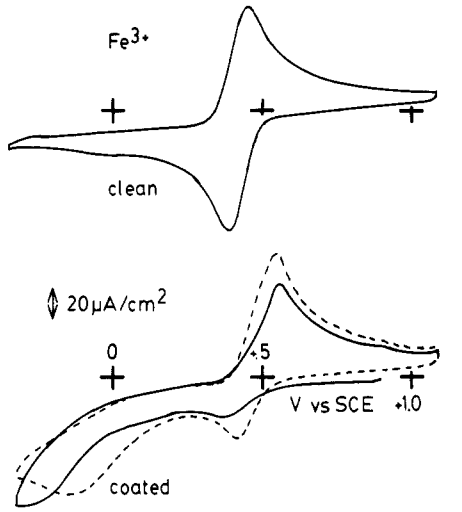

Figure 6. Cyclic voltammetry of a clean and a coated electrode. 0.7 mM Fe^{3+} in 0.5 M H_2SO_4; sweep rate 50 mV/s. Solid line, first scan; dashed line, second scan.

sputter at low beam power rapidly (ca. 3 min) removes all elements except gold (Figure 4B). Unfortunately, the lower frequency limit of the IR detector prevents confirmation of residual Si–Cl groups (normally located below 600 cm^{-1}).

Electrochemistry of the Coated Electrode. The monolayer appears to be unaffected by simple immersion in weakly acidic or neutral electrolytes, with or without potential control. Hydrogen evolution and gold oxidation occur close to the potentials found on a clean electrode, accompanied by abrupt changes in the wetting properties, i.e., water or hexadecane drops begin cling to the surface. The absence of inhibition of these faradaic processes suggests that water has ready access to the metal surface.

Cyclic voltammetry (Figures 5 and 6) of various electroactive ions (Fe^{2+}, Fe^{3+}, $Fe(CN)_6^{3-}$, $Fe(EDTA)^{2-}$, $Ru(NH_3)_6^{3+}$) with coated electrodes exhibit two common features: (1) attenuation of the peak currents relative to those obtained in the absence of a coating for both the forward and the reverse scans and (2) evolution of the voltammogram toward that of a clean electrode. The

Table I. Normalized Peak Currents and Peak Positions from LSV[a]

redox reactn	medium	i_{coated}/i_{clean}	$E_p^{coated} - E_p^{clean}$, V
$Fe^{+2} \rightarrow Fe^{+3} + e^-$	0.5 M H_2SO_4	0.085[b]	
		0.76	0.13
		0.43	0.17
		0.48	0.12
		0.47	0.16
		0.48	0.04
		0.76	0.04
		0.57	0.09
		0.53	0.00
		0.67	0.02
$Fe^{+3} + e^- \rightarrow Fe^{+2}$	0.5 M H_2SO_4	0.45	−0.05
		0.34	−0.05
		0.36	−0.06
		0.25	−0.02
		0.07	−0.04
		0.18	0.00
		0.04[b]	
$Fe(CN)_6^{4-} \rightarrow$	0.5 M H_2SO_4	0.20[b]	
$Fe(CN)_6^{3-} + e^-$		0.06[b]	
		0.47	0.18
		0.36	0.18
		0.58	0.05
		0.81	0.01
		0.83	0.03
		0.88	0.00
		0.47	0.03
		0.15[b]	
		0.38	0.00
$Fe(CN)_6^{4-} \rightarrow$	phosphate	0.49	0.00
$Fe(CN)_6^{3-} + e^-$	buffer pH 7		
$Fe(EDTA)^{2-} \rightarrow$	0.5 M Na_2SO_4	0.07[b]	
$Fe(EDTA)^- + e^-$	pH 3	0.10[b]	
$Fe(EDTA)^{2-} \rightarrow$	phosphate	0.03[b]	
$Fe(EDTA)^- + e^-$	buffer pH 6.5		
$Ru(NH_3)_6^{3+} + e^- \rightarrow$	phosphate	0.28	0.02
$Ru(NH_3)_6^{2+}$	buffer pH 6.5		

[a] Linear scan voltammograms were recorded at 50 mV/s; only data for the first scan are shown; the second peak for Fe^{+3} reduction is not listed. [b] Plateau currents.

greatest current attenuation always occurs on the first potential scan. The ratio of the initial peak currents for coated and clean electrodes (immersed in the same electrolyte to the same depth) is given in Table I. Ratio values vary between 0.03 and 0.9. Where the ratio drops below 0.2, the voltammogram exhibits a plateau rather than a peak shape (Figure 6). The peak potentials on coated electrodes is shifted to slightly larger overpotentials relative to those on a clean electrode (Table I). In all cases the second potential scan exhibits increased peak currents and the peak potentials shift toward those of the clean electrode voltammogram. The ferrous/ferric ion redox couple induces the most rapid change; also more rapid changes are observed on preanodized gold electrodes. The changes are irreversible and are occasionally accompanied by changes in the wetting properties of the electrode, i.e., increased hydrophilicity and oleophilicity.

Ferric ion reduction frequently display a second reduction peak at large overpotentials (0.5–1.0 V) (Figure 6).

Discussion

The present results indicate the formation of an oriented monolayer with a structural integrity due to a two-dimensional cross-linking of siloxy groups. Assembly of the monolayer by spontaneous adsorption compares favorably with the more complex Langmuir–Blodgett method, which cannot be used with hydrolytically sensitive molecules such as OTS.[35] The evidence indicates that part of the driving force for the formation of the monolayer assembly is at-

traction of the $SiCl_3$ head groups for a surface layer of water and the resultant stabilization by hydrolysis and cross-linking between head groups. The rapidity of monolayer assembly apparently excludes the growth of a random three-dimensional siloxane polymer on the surface even though polymer formation occurs elsewhere in the solution. Complete polymerization does not occur as evidenced by the presence of SiOH groups and some residual Cl. The film is quite stable toward solvent attack and is difficult to remove even in hot concentrated sulfuric acid. Faradaic processes rapidly destroy the integrity of the monolayer, as evidenced by the change in wetting properties and increase in currents with time. The disruption mechanism is unknown but may be attributed in part to the absence of covalent bonding between the OTS monolayer and the gold substrate.

Covalent anchoring of the monolayer to the gold substrate via an anodically formed oxide film is prevented by the facile reaction between the oxide and the $SiCl_3$ head groups. The reaction is rapid as an organized monolayer is formed on an anodized electrode within 5 min. These monolayers appear to be more permeable than the ones formed on oxide-free gold. Surface roughness does not seem to be the important factor causing the permeability difference since the pretreatment oxidation–reduction cycling, a procedure known to affect surface roughness, is the same for both oxide-coated and oxide-free samples. The most likely explanation then would seem to be that oxide–head group reaction products create defects in the monolayer. In contrast, part of the oxide layer is retained on a platinum substrate during OTS reaction and is readily reduced. The platinum electrode emerges wet after this reduction, indicating removal of the monolayer. Consequently, direct silanization of the substrate is not a viable approach for bonding organized monolayers to gold and platinum surfaces.

The monolayer is sufficiently thick (30 Å) that electron transfer by tunneling is anticipated to be extremely slow. Polymeropoulos and Sagiv[30] found a charge-transfer resistance of $8 \times 10^9\ \Omega$ for an OTS monolayer sandwiched between aluminum electrodes. Equating this with the electrochemical charge-transfer resistance leads to an exchange current of 3×10^{-12} A. At that level of exchange current, overpotentials of approximately 1 V are necessary to obtain significant currents. Ferric ion reduction is the only reaction for which a current peak is observed at large overpotentials, but there is no corresponding peak for ferrous ion oxidation at the equivalent positive overpotential. Therefore we believe that the initial cyclic voltammograms are indicative of a blocked electrode with defects in the blocking layer. The major sources of the defects are probably a combination of substrate surface roughness and incomplete head group polymerization. The redox ions migrate through these defects in the monolayer to be reduced or oxidized at the metal surface. Amatore et al.[53] have published the theory of cyclic voltammetry of a blocked electrode with microscopic active sites. Our voltammograms agree qualitatively with their predictions. As the active area of the direct sites decreases and the separation between the active sites increases, peak currents attenuate, and ultimately the voltammogram assumes a plateau shape with no sweep-rate dependence. The instability of the OTS monolayers during faradaic reactions precludes any sweep-rate study, but plateau-shaped voltammograms do appear for the greatest current attenuations. The variability of the initial peak current ratio in Table I indicates a poor reproducibility in the density and area of defects in OTS monolayers on metal. It also points out the extraordinary sensitivity of electrochemistry in detecting defects in an otherwise well-behaved monolayer.

This work point out one particular type of a two-dimensional molecular assembly which can function as an electrode blocking agent. Although this system is instructive it is clear that greater control of defect density and layer stability are desirable. Such control can be approached by variations in head group chemistry and work is now in progress toward this end in these laboratories.

Acknowledgment. Acknowledgement is made to the donors of the Petroleum Research Fund, administered by the American Chemical Society, for support of this research.

Registry No. OTS, 112-04-9; $Fe(CN)_6^{4-}$, 13408-63-4; $Ru(NH_3)_6^{3+}$, 18943-33-4; Fe, 7439-89-6; Au, 7440-57-5; hexane, 110-54-3.

(53) Amatore, C.; Saveant, J. M.; Tessier, D. *J. Electroanal. Chem.* **1983**, *147*, 39–51.